

Observation of New Resonances Decaying to $J/\psi K^+$ and $J/\psi \phi$

R. Aaij *et al.*^{*}
(LHCb Collaboration)



(Received 2 March 2021; accepted 7 July 2021; published 17 August 2021)

The first observation of exotic states with a new quark content $c\bar{c}u\bar{s}$ decaying to the $J/\psi K^+$ final state is reported with high significance from an amplitude analysis of the $B^+ \rightarrow J/\psi \phi K^+$ decay. The analysis is carried out using proton-proton collision data corresponding to a total integrated luminosity of 9 fb^{-1} collected by the LHCb experiment at center-of-mass energies of 7, 8, and 13 TeV. The most significant state, $Z_{cs}(4000)^+$, has a mass of $4003 \pm 6^{+4}_{-14} \text{ MeV}$, a width of $131 \pm 15 \pm 26 \text{ MeV}$, and spin parity $J^P = 1^+$, where the quoted uncertainties are statistical and systematic, respectively. A new $1^+ X(4685)$ state decaying to the $J/\psi \phi$ final state is also observed with high significance. In addition, the four previously reported $J/\psi \phi$ states are confirmed and two more exotic states, $Z_{cs}(4220)^+$ and $X(4630)$, are observed with significance exceeding 5 standard deviations.

DOI: 10.1103/PhysRevLett.127.082001

Charged states such as $Z_c(3900)^+$ [1,2] and $Z_c(4430)^+$ [3–5] provide evidence for exotic states, because light quarks are required to account for the nonzero electric charge in addition to the heavy quarkonium. (Charge conjugation is implied throughout this Letter.) Previously, only the u or d quarks were observed to constitute the light quark content of such charged exotic states, even though the existence of a Z_{cs} state as a strangeness-flavor partner of the $Z_c^+(3900)$ state had been predicted [6–10]. Recently, the BESIII experiment reported a 5.3 standard deviation (σ hereafter) observation of a threshold structure in the mass distribution of $D_s^- D^{*0} + D_s^{*-} D^0$ pairs produced in e^+e^- annihilation as recoil against a K^+ meson [11].

In this Letter, the first observation of two charged $Z_{cs}^+ \rightarrow J/\psi K^+$ states is reported from an updated amplitude analysis of the $B^+ \rightarrow J/\psi \phi K^+$ decay, as well as the observation of two more $X \rightarrow J/\psi \phi$ states. The analysis is based on the combined proton-proton (pp) collision data collected using the LHCb detector in run 1 at center-of-mass energies \sqrt{s} of 7 and 8 TeV, corresponding to a total integrated luminosity of 3 fb^{-1} , and in run 2 at $\sqrt{s} = 13 \text{ TeV}$, corresponding to an integrated luminosity of 6 fb^{-1} .

With run 1 data, LHCb performed the first amplitude analysis of the $B^+ \rightarrow J/\psi \phi K^+$ decay, investigating the $J/\psi \phi$ structure [12,13] in addition to the kaon excitations

(hereafter indicated as K^{*+}). The data were described with seven $K^{*+} \rightarrow \phi K^+$ resonances, four $X \rightarrow J/\psi \phi$ structures, and nonresonant (NR) ϕK^+ and $J/\psi \phi$ contributions. Four X structures, i.e., the $X(4140)$, $X(4274)$, $X(4500)$, and $X(4700)$ states, were observed [the recent Particle Data Group (PDG) convention labels these states as χ_{cJ} [14]]. Notably, the $X(4140)$ width was substantially larger than previously determined [15–17]. Only 3σ evidence for a $Z_{cs}^+ \rightarrow J/\psi K^+$ contribution was found [12,13].

The LHCb detector is a single-arm forward spectrometer covering the pseudorapidity range $2 < \eta < 5$, described in detail in Refs. [18,19]. Simulation is produced with software packages described in Refs. [20–23]. The $B^+ \rightarrow J/\psi(\rightarrow \mu^+\mu^-)\phi(\rightarrow K^+K^-)K^+$ signal candidates are first required to pass an online event selection performed by a trigger [24] dedicated for selecting J/ψ candidates. The signal decay is reconstructed by combining the J/ψ candidate with three kaon candidates with a total charge of one unit. The ϕ candidate is selected by requiring only one of two K^+K^- combinations to be consistent with the known ϕ mass [14] within $\pm 15 \text{ MeV}$. (Natural units with $\hbar = c = 1$ are used throughout.)

The off-line selection involves a loose preselection, followed by a multivariate classifier based on a gradient boosted decision tree (BDTG) [25,26]. The preselection is similar to that used in Refs. [12,13], but the requirement on the χ^2_{IP} of kaon candidates is loosened, where χ^2_{IP} is defined as the difference in the vertex fit χ^2 of the event primary pp collision vertex candidate, reconstructed with and without the particle considered. The BDTG response is constructed using eight variables exploring decay topology, particle momenta components transverse to the beam direction, and particle identification information (PID). The requirement on the BDTG response is chosen to maximize the signal significance multiplied by the purity [27].

*Full author list given at end of the article.

Published by the American Physical Society under the terms of the Creative Commons Attribution 4.0 International license. Further distribution of this work must maintain attribution to the author(s) and the published article's title, journal citation, and DOI. Funded by SCOAP³.

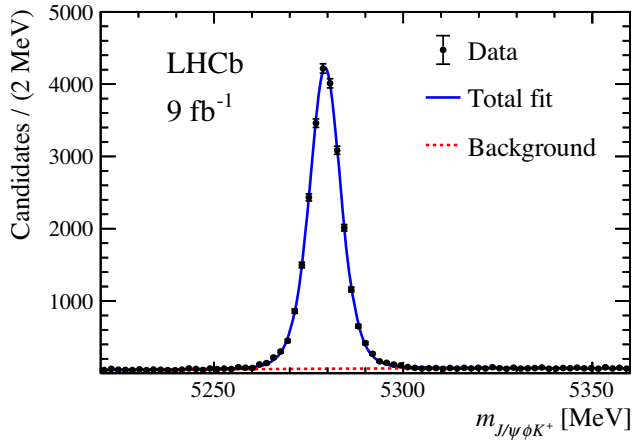


FIG. 1. Invariant-mass distribution of selected $B^+ \rightarrow J/\psi\phi K^+$ candidates with the fit overlaid.

The invariant-mass distribution of the $B^+ \rightarrow J/\psi\phi K^+$ candidates is shown in Fig. 1, fitted with the signal modeled by a Hypatia function [28] and the combinatorial background by a second-order polynomial function, yielding 24220 ± 170 signal candidates with a combinatorial-background fraction of 4.0% within a ± 15 MeV signal region. The region also includes an additional $\sim 2\%$ of non- ϕ $B^+ \rightarrow J/\psi K^+ K^- K^+$ background candidates, which are neglected in the amplitude model but considered in the evaluation of the systematic uncertainties. The candidates in the signal region are retained for further amplitude analysis. Compared to the previous run 1 analysis [12,13], the total signal yield is ~ 6 times larger, owing to a larger dataset and increase of 15% in signal efficiency due to the inclusion of PID in the BDTG classifier. The fraction of combinatorial background is almost a factor of 6 smaller, while that of the non- ϕ background is unchanged.

Figure 2 shows the Dalitz plots for $B^+ \rightarrow J/\psi\phi K^+$ candidates in the B^+ signal region. The most apparent features are four bands in the $J/\psi\phi$ mass distribution, corresponding to the previously reported $X(4140)$, $X(4274)$, $X(4500)$, and $X(4700)$ states. There is also a distinct band near 16 GeV^2 of the $J/\psi K^+$ mass squared.

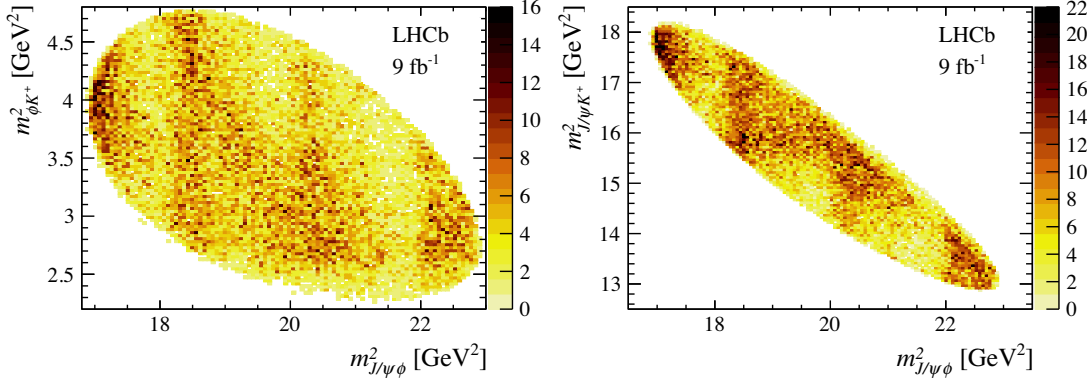


FIG. 2. Dalitz plots for $B^+ \rightarrow J/\psi\phi K^+$ candidates in a region ± 15 MeV around the B^+ mass peak.

To investigate the resonant structures, a full amplitude fit is performed using an unbinned maximum-likelihood method. The likelihood definition and the total probability density function (PDF), which includes a signal and a background component, are described in the previous publication [13]. Resonance line shapes are parametrized using the Breit-Wigner approximation. The signal B^+ decay is described in the helicity formalism by three decay chains: $K^{*+}(\rightarrow \phi K^+)J/\psi$, $X(\rightarrow J/\psi\phi)K^+$, and $Z_{cs}^+(\rightarrow J/\psi K^+)\phi$. Each chain is fully described by one mass and five angular observables. For example, the conventional K^{*+} chain has the following six observables $\Phi \equiv (m_{\phi K}, \theta_{K^*}, \theta_{J/\psi}, \theta_\phi, \Delta\phi_{K^*, J/\psi}, \Delta\phi_{K^*, \phi})$, where θ denotes the helicity angles and $\Delta\phi$ the angles between two decay planes. Because of the nonscalar final-state particles (μ^+ and μ^-), an azimuthal angle α_μ^i is required to align the helicity frames of μ^+ and μ^- between the chain i and the reference K^{*+} chain[4,5,29].

The model used in the previous study (run 1 model) is first tested. Because of the increased sample size, the model requires improvements (see Fig. 3 bottom row). Additional K^{*+} , X , and possible Z_{cs}^+ states are added until no further state with a significance larger than 5σ improves the overall fit. In total, nine K^{*+} , seven X , two Z_{cs}^+ , and one $J/\psi\phi$ NR components are taken as the default model, as listed in Table I. The nine K^{*+} states are all those with spin parity $J \leq 2$ and mass below 2 GeV, which are predicted by the relativistic potential model [30], and kinematically allowed, including three resonances with poles just below the ϕK^+ mass threshold. All components previously used in the run 1 model are included, but the $J^P = 1^+$ NR ϕK^+ and the broad 0^- state are replaced by the upper tails of $K_1(1400)$ and $K(1460)$ resonances, respectively. The newly added components are the upper tail of $1^- K^*(1410)$ resonance, $2^- X(4150)$, $1^+ X(4685)$, $1^- X(4630)$, $1^+ Z_{cs}(4000)^+$, and $Z_{cs}(4220)^+$ states.

Figure 3 shows the invariant-mass distributions for all pairs of final-state particles of the $B^+ \rightarrow J/\psi\phi K^+$ decay with fit projections from the amplitude analysis overlaid, for both the default model and the run 1 model. The fit

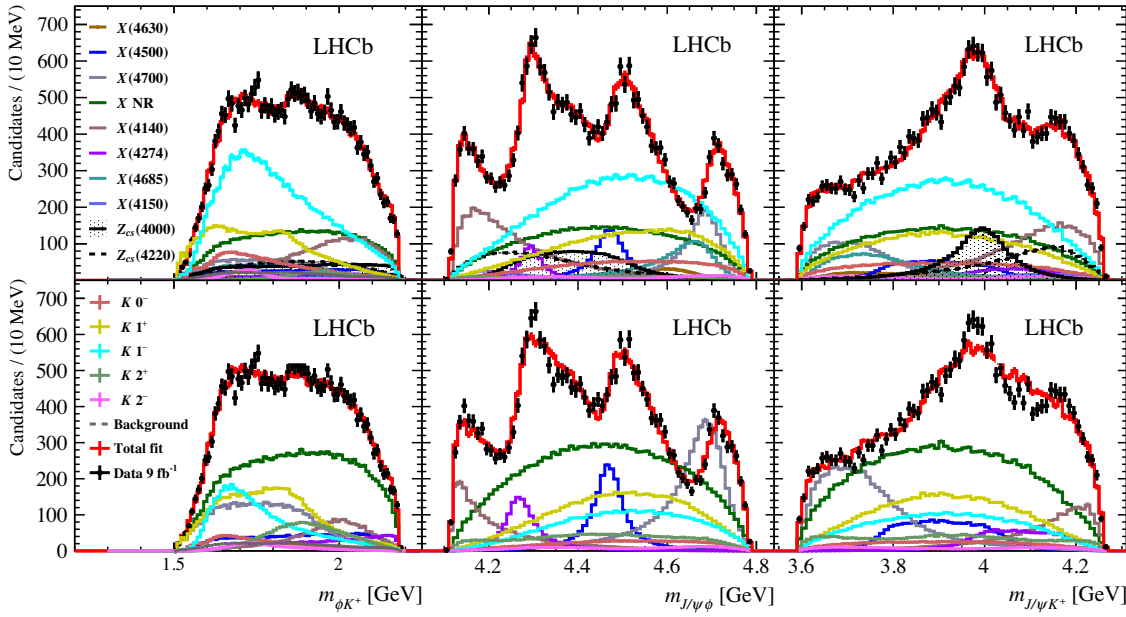


FIG. 3. Distributions of ϕK^+ (left), $J/\psi\phi$ (middle), and $J/\psi K^+$ (right) invariant masses for the $B^+ \rightarrow J/\psi\phi K^+$ candidates (black data points) compared with the fit results (red solid lines) of the default model (top row) and the run 1 model (bottom row).

results are summarized in Table I, including mass, width, fit fraction (FF), and significance of each component. The masses and widths of the four X states studied using the LHCb run 1 sample only are consistent with the previous

measurements [12,13]. The significance of each component is evaluated by assuming that the change of twice the log-likelihood between the default fit and the fit without this component follows a χ^2 distribution. The corresponding

TABLE I. Fit results from the default amplitude model. The significances are evaluated accounting for total (statistical) uncertainties. The listed masses and widths without uncertainties are taken from PDG [14] and are fixed in the fit. The listed world averages of the two K_2 and $K^*(1680)$ resonances do not contain the contributions from the previous LHCb run 1 results.

J^P	Contribution	Significance (σ)	M_0 (MeV)	Γ_0 (MeV)	FF (%)
1^+	2^1P_1	$K(1^+)$	$4.5 (4.5)$	$1861 \pm 10^{+16}_{-46}$	$149 \pm 41^{+231}_{-23}$
	2^3P_1	$K'(1^+)$	$4.5 (4.5)$	$1911 \pm 37^{+124}_{-48}$	$276 \pm 50^{+319}_{-159}$
2^-	1^3P_1	$K_1(1400)$	$9.2 (11)$	1403	174
2^-	1^1D_2	$K_2(1770)$	$7.9 (8.0)$	1773	186
1^-	1^3D_2	$K_2(1820)$	$5.8 (5.8)$	1816	276
1^-	1^3D_1	$K^*(1680)$	$4.7 (13)$	1717	322
2^-	2^3S_1	$K^*(1410)$	$7.7 (15)$	1414	232
2^-	2^3P_2	$K_2(1980)$	$1.6 (7.4)$	$1988 \pm 22^{+194}_{-31}$	$318 \pm 82^{+481}_{-101}$
0^-	2^1S_0	$K(1460)$	$12 (13)$	1483	336
2^-		$X(4150)$	$4.8 (8.7)$	$4146 \pm 18 \pm 33$	$135 \pm 28^{+59}_{-30}$
1^-		$X(4630)$	$5.5 (5.7)$	$4626 \pm 16^{+18}_{-110}$	$174 \pm 27^{+134}_{-73}$
0^+		$X(4500)$	$20 (20)$	$4474 \pm 3 \pm 3$	$77 \pm 6^{+10}_{-8}$
		$X(4700)$	$17 (18)$	$4694 \pm 4^{+16}_{-3}$	$87 \pm 8^{+16}_{-6}$
		$NR_{J/\psi\phi}$	$4.8 (5.7)$		$28 \pm 8^{+19}_{-11}$
1^+		$X(4140)$	$13 (16)$	$4118 \pm 11^{+19}_{-36}$	$162 \pm 21^{+24}_{-49}$
		$X(4274)$	$18 (18)$	$4294 \pm 4^{+3}_{-6}$	$53 \pm 5 \pm 5$
		$X(4685)$	$15 (15)$	$4684 \pm 7^{+13}_{-16}$	$126 \pm 15^{+37}_{-41}$
1^+		$Z_{cs}(4000)$	$15 (16)$	$4003 \pm 6^{+4}_{-14}$	$131 \pm 15 \pm 26$
		$Z_{cs}(4220)$	$5.9 (8.4)$	$4216 \pm 24^{+43}_{-30}$	$233 \pm 52^{+97}_{-73}$

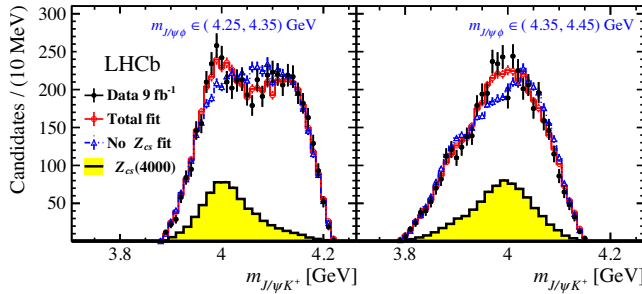


FIG. 4. Projections of the fits with the default model, performed in the full phase space, onto $m_{J/\psi K^+}$ in two slices of $m_{J/\psi\phi}$ with and without the 1^+ $Z_{cs}^+(4000)$ states. The narrow $Z_{cs}^+(4000)$ state at 4 GeV is evident.

number of degrees of freedom is equal to the reduction in the number of free parameters multiplied by a factor of 2 (1) when the mass and width of the component are floated (fixed) in the fit, which accounts for the look-elsewhere effect [13,31], as validated by pseudoexperiments. Figure 4 shows the $m_{J/\psi K^+}$ distributions in two slices of $m_{J/\psi\phi}$, which demonstrate the need for the narrower $Z_{cs}(4000)^+$ state. Including the 1^+ $Z_{cs}^+(4000)$ state improves the χ^2/n_{bin} from 84/35 to 43/35 (left slice) and from 79/37 to 32/37 (right slice), where n_{bin} is the number of nonzero bins.

The spin and parity of each exotic state is probed by testing alternative J^P hypotheses and comparing the fit likelihood values [13]. The J^P assignments for the previously reported four X states are confirmed with high significance. A 1^+ assignment is favored for the new $X(4685)$ state with also high significance, but the quantum numbers of the $X(4150)$ and $X(4630)$ are less well determined. The best hypothesis for the $X(4630)$ state is 1^- over 2^- at a 3σ level. The other hypotheses are ruled out by more than 5σ . The fit prefers 2^- for the $X(4150)$ state by more than 4σ . The narrower $Z_{cs}(4000)^+$ state is determined to be 1^+ with high significance. The broader $Z_{cs}(4220)^+$ state could be 1^+ or 1^- , with a 2σ difference in favor of the first hypothesis. Other spin-parity assignments are ruled out at 4.9σ level.

Systematic uncertainties are estimated for the masses, widths, and fit fractions of all states. To probe the effects from the neglected $B^+ \rightarrow J/\psi K^+ K^- K^+$ non- ϕ contributions, the ϕ mass window is changed from ± 15 to ± 7 MeV, and alternatively this background is subtracted using the *sPlot* technique [32]. The Blatt-Weisskopf barrier [13] hadron size is varied between 1.5 and 4.5 GeV^{-1} . The default NR 0^+ $J/\psi\phi$ representation is changed from a constant to a linear polynomial. Additional 1^+ or 2^+ NR $J/\psi\phi$ contributions are also included. The smallest allowed orbital angular momentum in the resonance function is varied. For the $X(4140)$, which peaks near the $J/\psi\phi$ threshold, the Flatté model [33] is used instead of the Breit-Wigner amplitude. A simplified one-channel K -matrix model [14] is used to describe various K^*

resonances instead of the sum of Breit-Wigner amplitudes. Two-channel K -matrix models have also been tried for the 2^1P_1 and 2^3P_1 K^* states with the coupled-channel thresholds opening up near 1.75 GeV, with an insignificant improvement to the description of the $m_{\phi K}$ distribution. To cover the full range of K^{*+} resonances predicted in the allowed ϕK^+ mass range, an extended model is tested by adding five more K^{*+} resonances with mass above 2 GeV [30]. The presence of an extra X state contribution, with J from 0 to 2, to the extended model is also checked. The difference between the results obtained from assigning 1^+ or 1^- hypotheses to the $Z_{cs}(4220)^+$ is taken as a systematic uncertainty. The mass-dependent width in the denominator of the Breit-Wigner function for the K^{*+} resonances is calculated with the lightest allowed channel (πK for natural spin-parity resonances and ωK for others) instead of ϕK .

The maximum deviation among the modeling uncertainties discussed above is summed in quadrature with the additional sources, including the uncertainties due to the fixed masses and widths of the known K^{*+} resonances, mismodeling of χ^2_{IP} of the B^+ candidate, background PDF model shape and fractions, and the finite size of the simulation samples. For the $Z_{cs}(4000)^+$ state, the largest systematic contribution is due to the J^P hypotheses of the $Z_{cs}(4220)^+$ state. The summary of fit results, including the systematic uncertainties, is listed in Table I. The smallest significance found when varying each of sources is taken as the significance accounting for systematic uncertainty.

Further evidence for the resonant character of $Z_{cs}(4000)^+$ is observed in Fig. 5, showing the evolution of the complex amplitude on the Argand diagram, obtained with the same method as previously reported for the $Z_c(4430)^-$ state [5]. The magnitude and phase have approximately circular evolution with $m_{J/\psi K^+}$ in the counterclockwise direction, as expected for a resonance.

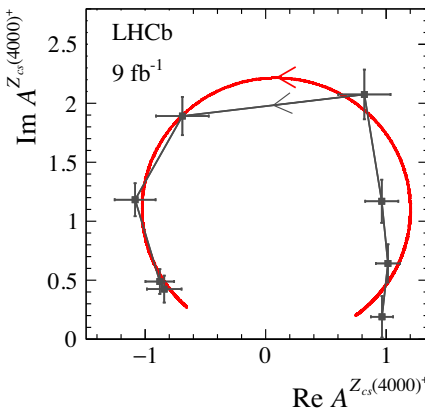


FIG. 5. Fitted values of the $Z_{cs}(4000)^+$ amplitude in eight $m_{J/\psi K^+}$ intervals, shown on an Argand diagram (black points). The red curve represents the expected Breit-Wigner behavior between $-1.4\Gamma_0$ and $1.4\Gamma_0$ around the $Z_{cs}(4000)^+$ mass.

The BESIII experiment reported observation of a $Z_{cs}(3985)^-$ resonance. Its mass $3982.5^{+1.8}_{-2.6}(\text{stat}) \pm 2.1(\text{syst})$ MeV is consistent with the $1^+ Z_{cs}(4000)^+$ state observed in this analysis, but with significantly narrower width $12.8^{+5.3}_{-4.4}(\text{stat}) \pm 3.0(\text{syst})$ MeV. When fixing the mass and width of this state to the nominal BESIII result in the amplitude fit to our data, twice the log-likelihood is worse by 160 units. The narrower width is also not supported by an alternative Flatté model with parameters obtained from our data. Therefore, there is no evidence that the $Z_{cs}(4000)^+$ state observed here is the same as the $Z_{cs}(3985)^-$ state observed by BESIII.

In conclusion, an improved full amplitude analysis of the $B^+ \rightarrow J/\psi\phi K^+$ decay is performed using 6 times larger signal yield than previously analyzed [12]. A relatively narrow $Z_{cs}(4000)^+$ state decaying to $J/\psi K^+$ with mass $4003 \pm 6(\text{stat})^{+4}_{-14}(\text{syst})$ MeV and width $131 \pm 15(\text{stat}) \pm 26(\text{syst})$ MeV is observed with large significance. Its spin parity is determined to be 1^+ also with high significance. A quasi-model-independent representation of the $Z_{cs}(4000)^+$ contribution in the fit shows a phase change in the amplitude consistent with that of a resonance. A broader 1^+ or $1^- Z_{cs}(4220)^+$ state is also required at 5.9σ . This is the first observation of states with hidden charm and strangeness that decay to the $J/\psi K^+$ final state. The four X states decaying to $J/\psi\phi$ observed in the run 1 analysis [12] are confirmed with higher significance, together with their quantum number assignments. An additional $1^+ X(4685)$ state is observed with relatively narrow width (about 125 MeV) with high significance. A new $X(4630)$ state is observed with a 5.5σ significance, with preferred 1^- over 2^- spin-parity assignment at 3σ level, and the other J^P hypotheses rejected at 5σ . This constitutes the first observation of exotic states with a new quark content $c\bar{c}u\bar{s}$ decaying to the $J/\psi K^+$ final state.

We express our gratitude to our colleagues in the CERN accelerator departments for the excellent performance of the LHC. We thank the technical and administrative staff at the LHCb institutes. We acknowledge support from CERN and from the following national agencies: CAPES, CNPq, FAPERJ, and FINEP (Brazil); MOST and NSFC (China); CNRS/IN2P3 (France); BMBF, DFG, and MPG (Germany); INFN (Italy); NWO (Netherlands); MNiSW and NCN (Poland); MEN/IFA (Romania); MSHE (Russia); MICINN (Spain); SNSF and SER (Switzerland); NASU (Ukraine); STFC (United Kingdom); DOE NP and NSF (U.S.). We acknowledge the computing resources that are provided by CERN, IN2P3 (France), KIT and DESY (Germany), INFN (Italy), SURF (Netherlands), PIC (Spain), GridPP (United Kingdom), RRCKI and Yandex LLC (Russia), CSCS (Switzerland), IFIN-HH (Romania), CBPF (Brazil), PL-GRID (Poland), and NERSC (U.S.). We are indebted to the communities behind the multiple open-source software packages on which we depend. Individual groups or members have received support from ARC and

ARDC (Australia); AvH Foundation (Germany); EPLANET, Marie Skłodowska-Curie Actions, and ERC (European Union); A*MIDEX, ANR, Labex P2IO and OCEVU, and Région Auvergne-Rhône-Alpes (France); Key Research Program of Frontier Sciences of CAS, CAS PIFI, CAS CCEPP, Fundamental Research Funds for the Central Universities, and Science and Technology Program of Guangzhou (China); RFBR, RSF, and Yandex LLC (Russia); GVA, XuntaGal, and GENCAT (Spain); the Leverhulme Trust, the Royal Society, and UKRI (United Kingdom).

- [1] M. Ablikim *et al.* (BESIII Collaboration), Observation of a Charged Charmoniumlike Structure in $e^+e^- \rightarrow \pi^+\pi^-J/\psi$ at $\sqrt{s} = 4.26$ GeV, *Phys. Rev. Lett.* **110**, 252001 (2013).
- [2] Z. Q. Liu *et al.* (Belle Collaboration), Study of $e^+e^- \rightarrow \pi^+\pi^-J/\psi$ and Observation of a Charged Charmoniumlike State at Belle, *Phys. Rev. Lett.* **110**, 252002 (2013).
- [3] S. K. Choi *et al.* (Belle Collaboration), Observation of a Resonance-Like Structure in the $\pi^\pm\psi'$ Mass Distribution in Exclusive $B \rightarrow K\pi^\pm\psi'$ Decays, *Phys. Rev. Lett.* **100**, 142001 (2008).
- [4] K. Chilikin *et al.* (Belle Collaboration), Experimental constraints on the spin and parity of the $Z(4430)^+$, *Phys. Rev. D* **88**, 074026 (2013).
- [5] R. Aaij *et al.* (LHCb Collaboration), Observation of the Resonant Character of the $Z(4430)^-$ State, *Phys. Rev. Lett.* **112**, 222002 (2014).
- [6] M. B. Voloshin, Strange hadrocharmonium, *Phys. Lett. B* **798**, 135022 (2019).
- [7] J. M. Dias, X. Liu, and M. Nielsen, Prediction for the decay width of a charged state near the $D_s\bar{D}^*/D_s^*\bar{D}$ threshold, *Phys. Rev. D* **88**, 096014 (2013).
- [8] D.-Y. Chen, X. Liu, and T. Matsuki, Predictions of Charged Charmoniumlike Structures with Hidden-Charm and Open-Strange Channels, *Phys. Rev. Lett.* **110**, 232001 (2013).
- [9] J. Ferretti and E. Santopinto, Hidden-charm and bottom tetra- and pentaquarks with strangeness in the hadroquarkonium and compact tetraquark models, *J. High Energy Phys.* **04** (2020) 119.
- [10] S. H. Lee, M. Nielsen, and U. Wiedner, D(s)D* molecule as an axial meson, *J. Korean Phys. Soc.* **55**, 424 (2009).
- [11] M. Ablikim *et al.* (BESIII Collaboration), Observation of a Near-Threshold Structure in the K^+ Recoil-Mass Spectra in $e^+e^- \rightarrow K^+(D_s^-D^{*0} + D_s^+D^0)$, *Phys. Rev. Lett.* **126**, 102001 (2021).
- [12] R. Aaij *et al.* (LHCb Collaboration), Observation of Exotic $J/\psi\phi$ Structures from Amplitude Analysis of $B^+ \rightarrow J/\psi\phi K^+$ Decays, *Phys. Rev. Lett.* **118**, 022003 (2017).
- [13] R. Aaij *et al.* (LHCb Collaboration), Amplitude analysis of $B^+ \rightarrow J/\psi\phi K^+$ decays, *Phys. Rev. D* **95**, 012002 (2017).
- [14] P. A. Zyla *et al.* (Particle Data Group), Review of particle physics, *Prog. Theor. Exp. Phys.* **2020**, 083C01 (2020).
- [15] T. Aaltonen *et al.* (CDF Collaboration), Evidence for a Narrow Near-Threshold Structure in the $J/\psi\phi$ Mass

- Spectrum in $B^+ \rightarrow J/\psi\phi K^+$ Decays, *Phys. Rev. Lett.* **102**, 242002 (2009).
- [16] T. Aaltonen *et al.* (CDF Collaboration), Observation of the $Y(4140)$ structure in the $J/\psi\phi$ mass spectrum in $B^\pm \rightarrow J/\psi\phi K^\pm$ decays, *Mod. Phys. Lett. A* **32**, 1750139 (2017).
- [17] S. Chatrchyan *et al.* (CMS Collaboration), Observation of a peaking structure in the $J/\psi\phi$ mass spectrum from $B^\pm \rightarrow J/\psi\phi K^\pm$ decays, *Phys. Lett. B* **734**, 261 (2014).
- [18] A. A. Alves Jr. *et al.* (LHCb Collaboration), The LHCb detector at the LHC, *J. Instrum.* **3**, S08005 (2008).
- [19] R. Aaij *et al.* (LHCb Collaboration), LHCb detector performance, *Int. J. Mod. Phys. A* **30**, 1530022 (2015).
- [20] T. Sjöstrand, S. Mrenna, and P. Skands, A brief introduction to PYTHIA 8.1, *Comput. Phys. Commun.* **178**, 852 (2008).
- [21] I. Belyaev *et al.*, Handling of the generation of primary events in Gauss, the LHCb simulation framework, *J. Phys. Conf. Ser.* **331**, 032047 (2011).
- [22] D. J. Lange, The EvtGen particle decay simulation package, *Nucl. Instrum. Methods Phys. Res., Sect. A* **462**, 152 (2001).
- [23] J. Allison *et al.* (Geant4 Collaboration), Geant4 developments and applications, *IEEE Trans. Nucl. Sci.* **53**, 270 (2006); S. Agostinelli *et al.* (Geant4 Collaboration), Geant4: A simulation toolkit, *Nucl. Instrum. Methods Phys. Res., Sect. A* **506**, 250 (2003).
- [24] R. Aaij *et al.*, The LHCb trigger and its performance in 2011, *J. Instrum.* **8**, P04022 (2013).
- [25] L. Breiman, J. H. Friedman, R. A. Olshen, and C. J. Stone, *Classification and Regression Trees* (Wadsworth International Group, Belmont, CA, 1984); H. Voss, A. Hoecker, J. Stelzer, and F. Tegenfeldt, TMVA—Toolkit for multivariate data analysis with ROOT, *Proc. Sci., ACAT2007* (2007) 040.
- [26] A. Hoecker *et al.*, TMVA 4—Toolkit for multivariate data analysis with ROOT. Users guide, [arXiv:physics/0703039](https://arxiv.org/abs/physics/0703039).
- [27] R. Aaij *et al.* (LHCb Collaboration), Amplitude analysis of $B_s^0 \rightarrow K_S^0 K^\pm \pi^\mp$ decays, *J. High Energy Phys.* **06** (2019) 114.
- [28] D. Martínez Santos and F. Dupertuis, Mass distributions marginalized over per-event errors, *Nucl. Instrum. Methods Phys. Res., Sect. A* **764**, 150 (2014).
- [29] R. Mizuk *et al.* (Belle Collaboration), Observation of two resonance-like structures in the $\pi^+\chi_{c1}$ mass distribution in exclusive $\bar{B}^0 \rightarrow K^-\pi^+\chi_{c1}$ decays, *Phys. Rev. D* **78**, 072004 (2008).
- [30] S. Godfrey and N. Isgur, Mesons in a relativized quark model with chromodynamics, *Phys. Rev. D* **32**, 189 (1985).
- [31] L. Lyons, Open statistical issues in particle physics, *Ann. Appl. Stat.* **2**, 887 (2008).
- [32] M. Pivk and F. R. Le Diberder, sPlot: A statistical tool to unfold data distributions, *Nucl. Instrum. Methods Phys. Res., Sect. A* **555**, 356 (2005).
- [33] S. M. Flatté, Coupled-channel analysis of the $\pi\eta$ and $K\bar{K}$ systems near $K\bar{K}$ threshold, *Phys. Lett.* **63B**, 224 (1976).

R. Aaij,³² C. Abellán Beteta,⁵⁰ T. Ackernley,⁶⁰ B. Adeua,⁴⁶ M. Adinolfi,⁵⁴ H. Afsharnia,⁹ C. A. Aidala,⁸⁵ S. Aiola,²⁵ Z. Ajaltouni,⁹ S. Akar,⁶⁵ J. Albrecht,¹⁵ F. Alessio,⁴⁸ M. Alexander,⁵⁹ A. Alfonso Albero,⁴⁵ Z. Aliouche,⁶² G. Alkhazov,³⁸ P. Alvarez Cartelle,⁵⁵ S. Amato,² Y. Amhis,¹¹ L. An,⁴⁸ L. Anderlini,²² A. Andreianov,³⁸ M. Andreotti,²¹ F. Archilli,¹⁷ A. Artamonov,⁴⁴ M. Artuso,⁶⁸ K. Arzymatov,⁴² E. Aslanides,¹⁰ M. Atzeni,⁵⁰ B. Audurier,¹² S. Bachmann,¹⁷ M. Bachmayer,⁴⁹ J. J. Back,⁵⁶ S. Baker,⁶¹ P. Baladron Rodriguez,⁴⁶ V. Balagura,¹² W. Baldini,^{21,48} J. Baptista Leite,¹ R. J. Barlow,⁶² S. Barsuk,¹¹ W. Barter,⁶¹ M. Bartolini,²⁴ F. Baryshnikov,⁸² J. M. Basels,¹⁴ G. Bassi,²⁹ B. Batsukh,⁶⁸ A. Battig,¹⁵ A. Bay,⁴⁹ M. Becker,¹⁵ F. Bedeschi,²⁹ I. Bediaga,¹ A. Beiter,⁶⁸ V. Belavin,⁴² S. Belin,²⁷ V. Bellee,⁴⁹ K. Belous,⁴⁴ I. Belov,⁴⁰ I. Belyaev,⁴¹ G. Bencivenni,²³ E. Ben-Haim,¹³ A. Berezhnyi,⁴⁰ R. Bernet,⁵⁰ D. Berninghoff,¹⁷ H. C. Bernstein,⁶⁸ C. Bertella,⁴⁸ A. Bertolin,²⁸ C. Betancourt,⁵⁰ F. Betti,^{20,d} Ia. Bezshyiko,⁵⁰ S. Bhasin,⁵⁴ J. Bhom,³⁵ L. Bian,⁷³ M. S. Bieker,¹⁵ S. Bifani,⁵³ P. Billoir,¹³ M. Birch,⁶¹ F. C. R. Bishop,⁵⁵ A. Bitadze,⁶² A. Bizzeti,^{22,k} M. Bjørn,⁶³ M. P. Blago,⁴⁸ T. Blake,⁵⁶ F. Blanc,⁴⁹ S. Blusk,⁶⁸ D. Bobulska,⁵⁹ J. A. Boelhauve,¹⁵ O. Boente Garcia,⁴⁶ T. Boettcher,⁶⁴ A. Boldyrev,⁸¹ A. Bondar,⁴³ N. Bondar,^{38,48} S. Borghi,⁶² M. Borisjak,⁴² M. Borsato,¹⁷ J. T. Borsuk,³⁵ S. A. Bouchiba,⁴⁹ T. J. V. Bowcock,⁶⁰ A. Boyer,⁴⁸ C. Bozzi,²¹ M. J. Bradley,⁶¹ S. Braun,⁶⁶ A. Brea Rodriguez,⁴⁶ M. Brodski,⁴⁸ J. Brodzicka,³⁵ A. Brossa Gonzalo,⁵⁶ D. Brundu,²⁷ A. Buonaura,⁵⁰ C. Burr,⁴⁸ A. Bursche,²⁷ A. Butkevich,³⁹ J. S. Butter,³² J. Buytaert,⁴⁸ W. Byczynski,⁴⁸ S. Cadeddu,²⁷ H. Cai,⁷³ R. Calabrese,^{21,f} L. Calefice,^{15,13} L. Calero Diaz,²³ S. Cali,²³ R. Calladine,⁵³ M. Calvi,^{26,j} M. Calvo Gomez,⁸⁴ P. Camargo Magalhaes,⁵⁴ A. Camboni,^{45,84} P. Campana,²³ A. F. Campoverde Quezada,⁶ S. Capelli,^{26,j} L. Capriotti,^{20,d} A. Carbone,^{20,d} G. Carboni,³¹ R. Cardinale,^{24,h} A. Cardini,²⁷ I. Carli,⁴ P. Carniti,^{26,j} L. Carus,¹⁴ K. Carvalho Akiba,³² A. Casais Vidal,⁴⁶ G. Casse,⁶⁰ M. Cattaneo,⁴⁸ G. Cavallero,⁴⁸ S. Celani,⁴⁹ J. Cerasoli,¹⁰ A. J. Chadwick,⁶⁰ M. G. Chapman,⁵⁴ M. Charles,¹³ Ph. Charpentier,⁴⁸ G. Chatzikonstantinidis,⁵³ C. A. Chavez Barajas,⁶⁰ M. Chefdeville,⁸ C. Chen,³ S. Chen,²⁷ A. Chernov,³⁵ V. Chobanova,⁴⁶ S. Cholak,⁴⁹ M. Chrzaszcz,³⁵ A. Chubykin,³⁸ V. Chulikov,³⁸ P. Ciambrone,²³ M. F. Cicala,⁵⁶ X. Cid Vidal,⁴⁶ G. Ciezarek,⁴⁸ P. E. L. Clarke,⁵⁸ M. Clemencic,⁴⁸ H. V. Cliff,⁵⁵ J. Closier,⁴⁸ J. L. Cobbledick,⁶² V. Coco,⁴⁸ J. A. B. Coelho,¹¹ J. Cogan,¹⁰ E. Cogneras,⁹ L. Cojocariu,³⁷ P. Collins,⁴⁸ T. Colombo,⁴⁸ L. Congedo,^{19,c} A. Contu,²⁷ N. Cooke,⁵³ G. Coombs,⁵⁹ G. Corti,⁴⁸ C. M. Costa Sobral,⁵⁶ B. Couturier,⁴⁸ D. C. Craik,⁶⁴ J. Crkovská,⁶⁷ M. Cruz Torres,¹ R. Currie,⁵⁸ C. L. Da Silva,⁶⁷ E. Dall'Occo,¹⁵ J. Dalseno,⁴⁶ C. D'Ambrosio,⁴⁸

- A. Danilina,⁴¹ P. d'Argent,⁴⁸ A. Davis,⁶² O. De Aguiar Francisco,⁶² K. De Bruyn,⁷⁸ S. De Capua,⁶² M. De Cian,⁴⁹ J. M. De Miranda,¹ L. De Paula,² M. De Serio,^{19,c} D. De Simone,⁵⁰ P. De Simone,²³ J. A. de Vries,⁷⁹ C. T. Dean,⁶⁷ D. Decamp,⁸ L. Del Buono,¹³ B. Delaney,⁵⁵ H.-P. Dembinski,¹⁵ A. Dendek,³⁴ V. Denysenko,⁵⁰ D. Derkach,⁸¹ O. Deschamps,⁹ F. Desse,¹¹ F. Dettori,^{27,e} B. Dey,⁷³ P. Di Nezza,²³ S. Didenko,⁸² L. Dieste Maronas,⁴⁶ H. Dijkstra,⁴⁸ V. Dobishuk,⁵² A. M. Donohoe,¹⁸ F. Dordei,²⁷ A. C. dos Reis,¹ L. Douglas,⁵⁹ A. Dovbnya,⁵¹ A. G. Downes,⁸ K. Dreimanis,⁶⁰ M. W. Dudek,³⁵ L. Dufour,⁴⁸ V. Duk,⁷⁷ P. Durante,⁴⁸ J. M. Durham,⁶⁷ D. Dutta,⁶² M. Dziewiecki,¹⁷ A. Dziurda,³⁵ A. Dzyuba,³⁸ S. Easo,⁵⁷ U. Egede,⁶⁹ V. Egorychev,⁴¹ S. Eidelman,^{43,v} S. Eisenhardt,⁵⁸ S. Ek-In,⁴⁹ L. Eklund,^{59,w} S. Ely,⁶⁸ A. Ene,³⁷ E. Epple,⁶⁷ S. Escher,¹⁴ J. Eschle,⁵⁰ S. Esen,³² T. Evans,⁴⁸ A. Falabella,²⁰ J. Fan,³ Y. Fan,⁶ B. Fang,⁷³ S. Farry,⁶⁰ D. Fazzini,^{26,j} P. Fedin,⁴¹ M. Féo,⁴⁸ P. Fernandez Declara,⁴⁸ A. Fernandez Prieto,⁴⁶ J. M. Fernandez-tenllado Arribas,⁴⁵ F. Ferrari,^{20,d} L. Ferreira Lopes,⁴⁹ F. Ferreira Rodrigues,² S. Ferreres Sole,³² M. Ferrillo,⁵⁰ M. Ferro-Luzzi,⁴⁸ S. Filippov,³⁹ R. A. Fini,¹⁹ M. Fiorini,^{21,f} M. Firlej,³⁴ K. M. Fischer,⁶³ C. Fitzpatrick,⁶² T. Fiutowski,³⁴ F. Fleuret,¹² M. Fontana,¹³ F. Fontanelli,^{24,h} R. Forty,⁴⁸ V. Franco Lima,⁶⁰ M. Franco Sevilla,⁶⁶ M. Frank,⁴⁸ E. Franzoso,²¹ G. Frau,¹⁷ C. Frei,⁴⁸ D. A. Friday,⁵⁹ J. Fu,²⁵ Q. Fuehring,¹⁵ W. Funk,⁴⁸ E. Gabriel,³² T. Gaintseva,⁴² A. Gallas Torreira,⁴⁶ D. Galli,^{20,d} S. Gambetta,^{58,48} Y. Gan,³ M. Gandelman,² P. Gandini,²⁵ Y. Gao,⁵ M. Garau,²⁷ L. M. Garcia Martin,⁵⁶ P. Garcia Moreno,⁴⁵ J. García Pardiñas,^{26,j} B. Garcia Plana,⁴⁶ F. A. Garcia Rosales,¹² L. Garrido,⁴⁵ C. Gaspar,⁴⁸ R. E. Geertsema,³² D. Gerick,¹⁷ L. L. Gerken,¹⁵ E. Gersabeck,⁶² M. Gersabeck,⁶² T. Gershon,⁵⁶ D. Gerstel,¹⁰ Ph. Ghez,⁸ V. Gibson,⁵⁵ H. K. Giemza,³⁶ M. Giovannetti,^{23,p} A. Gioventù,⁴⁶ P. Gironella Gironell,⁴⁵ L. Giubega,³⁷ C. Giugliano,^{21,48,f} K. Gizdov,⁵⁸ E. L. Gkougkousis,⁴⁸ V. V. Gligorov,¹³ C. Göbel,⁷⁰ E. Golobardes,⁸⁴ D. Golubkov,⁴¹ A. Golutvin,^{61,82} A. Gomes,^{1,a} S. Gomez Fernandez,⁴⁵ F. Goncalves Abrantes,⁶³ M. Goncerz,³⁵ G. Gong,³ P. Gorbounov,⁴¹ I. V. Gorelov,⁴⁰ C. Gotti,²⁶ E. Govorkova,⁴⁸ J. P. Grabowski,¹⁷ R. Graciani Diaz,⁴⁵ T. Grammatico,¹³ L. A. Granado Cardoso,⁴⁸ E. Graugés,⁴⁵ E. Graverini,⁴⁹ G. Graziani,²² A. Grecu,³⁷ L. M. Greeven,³² P. Griffith,^{21,f} L. Grillo,⁶² S. Gromov,⁸² B. R. Gruberg Cazon,⁶³ C. Gu,³ M. Guarise,²¹ P. A. Günther,¹⁷ E. Gushchin,³⁹ A. Guth,¹⁴ Y. Guz,^{44,48} T. Gys,⁴⁸ T. Hadavizadeh,⁶⁹ G. Haefeli,⁴⁹ C. Haen,⁴⁸ J. Haimberger,⁴⁸ T. Halewood-leagas,⁶⁰ P. M. Hamilton,⁶⁶ Q. Han,⁷ X. Han,¹⁷ T. H. Hancock,⁶³ S. Hansmann-Menzemer,¹⁷ N. Harnew,⁶³ T. Harrison,⁶⁰ C. Hasse,⁴⁸ M. Hatch,⁴⁸ J. He,^{6,b} M. Hecker,⁶¹ K. Heijhoff,³² K. Heinicke,¹⁵ A. M. Hennequin,⁴⁸ K. Hennessy,⁶⁰ L. Henry,^{25,47} J. Heuel,¹⁴ A. Hicheur,² D. Hill,⁴⁹ M. Hilton,⁶² S. E. Hollitt,¹⁵ J. Hu,¹⁷ J. Hu,⁷² W. Hu,⁷ W. Huang,⁶ X. Huang,⁷³ W. Hulsbergen,³² R. J. Hunter,⁵⁶ M. Hushchyn,⁸¹ D. Hutchcroft,⁶⁰ D. Hynds,³² P. Ibis,¹⁵ M. Idzik,³⁴ D. Ilin,³⁸ P. Ilten,⁶⁵ A. Inglessi,³⁸ A. Ishteev,⁸² K. Ivshin,³⁸ R. Jacobsson,⁴⁸ S. Jakobsen,⁴⁸ E. Jans,³² B. K. Jashal,⁴⁷ A. Jawahery,⁶⁶ V. Jevtic,¹⁵ M. Jezabek,³⁵ F. Jiang,³ M. John,⁶³ D. Johnson,⁴⁸ C. R. Jones,⁵⁵ T. P. Jones,⁵⁶ B. Jost,⁴⁸ N. Jurik,⁴⁸ S. Kandybei,⁵¹ Y. Kang,³ M. Karacson,⁴⁸ M. Karpov,⁸¹ N. Kazeev,⁸¹ F. Keizer,^{55,48} M. Kenzie,⁵⁶ T. Ketel,³³ B. Khanji,¹⁵ A. Kharisova,⁸³ S. Kholodenko,⁴⁴ K. E. Kim,⁶⁸ T. Kirn,¹⁴ V. S. Kirsebom,⁴⁹ O. Kitouni,⁶⁴ S. Klaver,³² K. Klimaszewski,³⁶ S. Koliiev,⁵² A. Kondybayeva,⁸² A. Konoplyannikov,⁴¹ P. Kopciewicz,³⁴ R. Kopecna,¹⁷ P. Koppenburg,³² M. Korolev,⁴⁰ I. Kostiuk,^{32,52} O. Kot,⁵² S. Kotriakhova,^{38,30} P. Kravchenko,³⁸ L. Kravchuk,³⁹ R. D. Krawczyk,⁴⁸ M. Kreps,⁵⁶ F. Kress,⁶¹ S. Kretzschmar,¹⁴ P. Krokovny,^{43,v} W. Krupa,³⁴ W. Krzemien,³⁶ W. Kucewicz,^{35,t} M. Kucharczyk,³⁵ V. Kudryavtsev,^{43,v} H. S. Kuindersma,³² G. J. Kunde,⁶⁷ T. Kvaratskheliya,⁴¹ D. Lacarrere,⁴⁸ G. Lafferty,⁶² A. Lai,²⁷ A. Lampis,²⁷ D. Lancierini,⁵⁰ J. J. Lane,⁶² R. Lane,⁵⁴ G. Lanfranchi,²³ C. Langenbruch,¹⁴ J. Langer,¹⁵ O. Lantwin,^{50,82} T. Latham,⁵⁶ F. Lazzari,^{29,q} R. Le Gac,¹⁰ S. H. Lee,⁸⁵ R. Lefèvre,⁹ A. Leflat,⁴⁰ S. Legotin,⁸² O. Leroy,¹⁰ T. Lesiak,³⁵ B. Leverington,¹⁷ H. Li,⁷² L. Li,⁶³ P. Li,¹⁷ Y. Li,⁴ Y. Li,⁴ Z. Li,⁶⁸ X. Liang,⁶¹ T. Lin,⁴⁸ R. Lindner,²⁷ V. Lisovskyi,¹⁵ R. Litvinov,²⁷ G. Liu,⁷² H. Liu,⁶ S. Liu,⁴ X. Liu,³ A. Loi,²⁷ J. Lomba Castro,⁴⁶ I. Longstaff,⁵⁹ J. H. Lopes,² G. H. Lovell,⁵⁵ Y. Lu,⁴ D. Lucchesi,^{28,l} S. Luchuk,³⁹ M. Lucio Martinez,³² V. Lukashenko,³² Y. Luo,³ A. Lupato,⁶² E. Luppi,^{21,f} O. Lupton,⁵⁶ A. Lusiani,^{29,m} X. Lyu,⁶ L. Ma,⁴ S. Maccolini,^{20,d} F. Machefert,¹¹ F. Maciuc,³⁷ V. Macko,⁴⁹ P. Mackowiak,¹⁵ S. Maddrell-Mander,⁵⁴ O. Madejczyk,³⁴ L. R. Madhan Mohan,⁵⁴ O. Maev,³⁸ A. Maevskiy,⁸¹ D. Maisuzenko,³⁸ M. W. Majewski,³⁴ J. J. Malczewski,³⁵ S. Malde,⁶³ B. Malecki,⁴⁸ A. Malinin,⁸⁰ T. Maltsev,^{43,v} H. Malygina,¹⁷ G. Manca,^{27,e} G. Mancinelli,¹⁰ R. Manera Escalero,⁴⁵ D. Manuzzi,^{20,d} D. Marangotto,^{25,i} J. Maratas,^{9,s} J. F. Marchand,⁸ U. Marconi,²⁰ S. Mariani,^{22,48,g} C. Marin Benito,¹¹ M. Marinangeli,⁴⁹ P. Marino,^{49,m} J. Marks,¹⁷ P. J. Marshall,⁶⁰ G. Martellotti,³⁰ L. Martinazzoli,^{48,j} M. Martinelli,^{26,j} D. Martinez Santos,⁴⁶ F. Martinez Vidal,⁴⁷ A. Massafferri,¹ M. Materok,¹⁴ R. Matev,⁴⁸ A. Mathad,⁵⁰ Z. Mathe,⁴⁸ V. Matiunin,⁴¹ C. Matteuzzi,²⁶ K. R. Mattioli,⁸⁵ A. Mauri,³² E. Maurice,¹² J. Mauricio,⁴⁵ M. Mazurek,³⁶ M. McCann,⁶¹ L. Mcconnell,¹⁸ T. H. McGrath,⁶² A. McNab,⁶² R. McNulty,¹⁸ J. V. Mead,⁶⁰ B. Meadows,⁶⁵ C. Meaux,¹⁰ G. Meier,¹⁵ N. Meinert,⁷⁶ D. Melnychuk,³⁶ S. Meloni,^{26,j} M. Merk,^{32,79} A. Merli,²⁵ L. Meyer Garcia,² M. Mikhasenko,⁴⁸ D. A. Milanes,⁷⁴ E. Millard,⁵⁶ M. Milovanovic,⁴⁸

- M.-N. Minard,⁸ L. Minzoni,^{21,f} S. E. Mitchell,⁵⁸ B. Mitreska,⁶² D. S. Mitzel,⁴⁸ A. Mödden,¹⁵ R. A. Mohammed,⁶³ R. D. Moise,⁶¹ T. Mombächer,¹⁵ I. A. Monroy,⁷⁴ S. Monteil,⁹ M. Morandin,²⁸ G. Morello,²³ M. J. Morello,^{29,m} J. Moron,³⁴ A. B. Morris,⁷⁵ A. G. Morris,⁵⁶ R. Mountain,⁶⁸ H. Mu,³ F. Muheim,^{58,48} M. Mukherjee,⁷ M. Mulder,⁴⁸ D. Müller,⁴⁸ K. Müller,⁵⁰ C. H. Murphy,⁶³ D. Murray,⁶² P. Muzzetto,^{27,48} P. Naik,⁵⁴ T. Nakada,⁴⁹ R. Nandakumar,⁵⁷ T. Nanut,⁴⁹ I. Nasteva,² M. Needham,⁵⁸ I. Neri,²¹ N. Neri,^{25,i} S. Neubert,⁷⁵ N. Neufeld,⁴⁸ R. Newcombe,⁶¹ T. D. Nguyen,⁴⁹ C. Nguyen-Mau,^{49,x} E. M. Niel,¹¹ S. Nieswand,¹⁴ N. Nikitin,⁴⁰ N. S. Nolte,⁴⁸ C. Nunez,⁸⁵ A. Oblakowska-Mucha,³⁴ V. Obraztsov,⁴⁴ D. P. O'Hanlon,⁵⁴ R. Oldeman,^{27,e} M. E. Olivares,⁶⁸ C. J. G. Onderwater,⁷⁸ A. Ossowska,³⁵ J. M. Otalora Goicochea,² T. Ovsiannikova,⁴¹ P. Owen,⁵⁰ A. Oyanguren,⁴⁷ B. Pagare,⁵⁶ P. R. Pais,⁴⁸ T. Pajero,^{29,48,m} A. Palano,¹⁹ M. Palutan,²³ Y. Pan,⁶² G. Panshin,⁸³ A. Papanestis,⁵⁷ M. Pappagallo,^{19,c} L. L. Pappalardo,^{21,f} C. Pappenheimer,⁶⁵ W. Parker,⁶⁶ C. Parkes,⁶² C. J. Parkinson,⁴⁶ B. Passalacqua,²¹ G. Passaleva,²² A. Pastore,¹⁹ M. Patel,⁶¹ C. Patrignani,^{20,d} C. J. Pawley,⁷⁹ A. Pearce,⁴⁸ A. Pellegrino,³² M. Pepe Altarelli,⁴⁸ S. Perazzini,²⁰ D. Pereima,⁴¹ P. Perret,⁹ K. Petridis,⁵⁴ A. Petrolini,^{24,h} A. Petrov,⁸⁰ S. Petrucci,⁵⁸ M. Petruzzo,²⁵ T. T. H. Pham,⁶⁸ A. Philippov,⁴² L. Pica,^{29,n} M. Piccini,⁷⁷ B. Pietrzyk,⁸ G. Pietrzyk,⁴⁹ M. Pili,⁶³ D. Pinci,³⁰ F. Pisani,⁴⁸ A. Piucci,¹⁷ Resmi P. K.,¹⁰ V. Placinta,³⁷ J. Plews,⁵³ M. Plo Casasus,⁴⁶ F. Polci,¹³ M. Poli Lener,²³ M. Poliakova,⁶⁸ A. Poluektov,¹⁰ N. Polukhina,^{82,u} I. Polyakov,⁶⁸ E. Polycarpo,² G. J. Pomery,⁵⁴ S. Ponce,⁴⁸ D. Popov,^{6,48} S. Popov,⁴² S. Poslavskii,⁴⁴ K. Prasant,³⁵ L. Promberger,⁴⁸ C. Prouve,⁴⁶ V. Pugatch,⁵² H. Pullen,⁶³ G. Punzi,^{29,n} W. Qian,⁶ J. Qin,⁶ R. Quagliani,¹³ B. Quintana,⁸ N. V. Raab,¹⁸ R. I. Rabadan Trejo,¹⁰ B. Rachwal,³⁴ J. H. Rademacker,⁵⁴ M. Rama,²⁹ M. Ramos Pernas,⁵⁶ M. S. Rangel,² F. Ratnikov,^{42,81} G. Raven,³³ M. Reboud,⁸ F. Redi,⁴⁹ F. Reiss,¹³ C. Remon Alepuz,⁴⁷ Z. Ren,³ V. Renaudin,⁶³ R. Ribatti,²⁹ S. Ricciardi,⁵⁷ K. Rinnert,⁶⁰ P. Robbe,¹¹ A. Robert,¹³ G. Robertson,⁵⁸ A. B. Rodrigues,⁴⁹ E. Rodrigues,⁶⁰ J. A. Rodriguez Lopez,⁷⁴ A. Rollings,⁶³ P. Roloff,⁴⁸ V. Romanovskiy,⁴⁴ M. Romero Lamas,⁴⁶ A. Romero Vidal,⁴⁶ J. D. Roth,⁸⁵ M. Rotondo,²³ M. S. Rudolph,⁶⁸ T. Ruf,⁴⁸ J. Ruiz Vidal,⁴⁷ A. Ryzhikov,⁸¹ J. Ryzka,³⁴ J. J. Saborido Silva,⁴⁶ N. Sagidova,³⁸ N. Sahoo,⁵⁶ B. Saitta,^{27,e} D. Sanchez Gonzalo,⁴⁵ C. Sanchez Gras,³² R. Santacesaria,³⁰ C. Santamarina Rios,⁴⁶ M. Santimaria,²³ E. Santovetti,^{31,p} D. Saranin,⁸² G. Sarpis,⁵⁹ M. Sarpis,⁷⁵ A. Sarti,³⁰ C. Satriano,^{30,o} A. Satta,³¹ M. Saur,¹⁵ D. Savrina,^{41,40} H. Sazak,⁹ L. G. Scantlebury Smead,⁶³ S. Schael,¹⁴ M. Schellenberg,¹⁵ M. Schiller,⁵⁹ H. Schindler,⁴⁸ M. Schmelling,¹⁶ B. Schmidt,⁴⁸ O. Schneider,⁴⁹ A. Schopper,⁴⁸ M. Schubiger,³² S. Schulte,⁴⁹ M. H. Schune,¹¹ R. Schwemmer,⁴⁸ B. Sciascia,²³ A. Sciubba,²³ S. Sellam,⁴⁶ A. Semennikov,⁴¹ M. Senghi Soares,³³ A. Sergi,^{24,48} N. Serra,⁵⁰ L. Sestini,²⁸ A. Seuthe,¹⁵ P. Seyfert,⁴⁸ D. M. Shangase,⁸⁵ M. Shapkin,⁴⁴ I. Shchemerov,⁸² L. Shchutska,⁴⁹ T. Shears,⁶⁰ L. Shekhtman,^{43,v} Z. Shen,⁵ V. Shevchenko,⁸⁰ E. B. Shields,^{26,j} E. Shmanin,⁸² J. D. Shupperd,⁶⁸ B. G. Siddi,²¹ R. Silva Coutinho,⁵⁰ G. Simi,²⁸ S. Simone,^{19,c} N. Skidmore,⁶² T. Skwarnicki,⁶⁸ M. W. Slater,⁵³ I. Slazyk,^{21,f} J. C. Smallwood,⁶³ J. G. Smeaton,⁵⁵ A. Smetkina,⁴¹ E. Smith,¹⁴ M. Smith,⁶¹ A. Snoch,³² M. Soares,²⁰ L. Soares Lavra,⁹ M. D. Sokoloff,⁶⁵ F. J. P. Soler,⁵⁹ A. Solovev,³⁸ I. Solovyev,³⁸ F. L. Souza De Almeida,² B. Souza De Paula,² B. Spaan,¹⁵ E. Spadaro Norella,^{25,i} P. Spradlin,⁵⁹ F. Stagni,⁴⁸ M. Stahl,⁶⁵ S. Stahl,⁴⁸ P. Stefkó,⁴⁹ O. Steinkamp,^{50,82} S. Stemmle,¹⁷ O. Stenyakin,⁴⁴ H. Stevens,¹⁵ S. Stone,⁶⁸ M. E. Stramaglia,⁴⁹ M. Stratciuc,³⁷ D. Strekalina,⁸² F. Suljik,⁶³ J. Sun,²⁷ L. Sun,⁷³ Y. Sun,⁶⁶ P. Svihra,⁶² P. N. Swallow,⁵³ K. Swientek,³⁴ A. Szabelski,³⁶ T. Szumlak,³⁴ M. Szymanski,⁴⁸ S. Taneja,⁶² F. Teubert,⁴⁸ E. Thomas,⁶⁰ K. A. Thomson,⁶⁰ M. J. Tilley,⁶¹ V. Tisserand,⁹ S. T'Jampens,⁸ M. Tobin,⁴ S. Tolk,⁴⁸ L. Tomassetti,^{21,f} D. Torres Machado,¹ D. Y. Tou,¹³ M. Traill,⁵⁹ M. T. Tran,⁴⁹ E. Trifonova,⁸² C. Trippi,⁴⁹ G. Tuci,^{29,n} A. Tully,⁴⁹ N. Tuning,³² A. Ukleja,³⁶ D. J. Unverzagt,¹⁷ E. Ursov,⁸² A. Usachov,³² A. Ustyuzhanin,^{42,81} U. Uwer,¹⁷ A. Wagner,⁸³ V. Vagnoni,²⁰ A. Valassi,⁴⁸ G. Valenti,²⁰ N. Valls Canudas,⁴⁵ M. van Beuzekom,³² M. Van Dijk,⁴⁹ E. van Herwijnen,⁸² C. B. Van Hulse,¹⁸ M. van Veghel,⁷⁸ R. Vazquez Gomez,⁴⁶ P. Vazquez Regueiro,⁴⁶ C. Vázquez Sierra,⁴⁸ S. Vecchi,²¹ J. J. Velthuis,⁵⁴ M. Veltri,^{22,r} A. Venkateswaran,⁶⁸ M. Veronesi,³² M. Vesterinen,⁵⁶ D. Vieira,⁶⁵ M. Vieites Diaz,⁴⁹ H. Viemann,⁷⁶ X. Vilasis-Cardona,⁸⁴ E. Vilella Figueras,⁶⁰ P. Vincent,¹³ G. Vitali,²⁹ A. Vollhardt,⁵⁰ D. Vom Bruch,¹⁰ A. Vorobyev,³⁸ V. Vorobyev,^{43,v} N. Voropaev,³⁸ R. Waldi,⁷⁶ J. Walsh,²⁹ C. Wang,¹⁷ J. Wang,⁵ J. Wang,⁴ J. Wang,³ J. Wang,⁷³ M. Wang,³ R. Wang,⁵⁴ Y. Wang,⁷ Z. Wang,⁵⁰ H. M. Wark,⁶⁰ N. K. Watson,⁵³ S. G. Weber,¹³ D. Websdale,⁶¹ C. Weisser,⁶⁴ B. D. C. Westhenry,⁵⁴ D. J. White,⁶² M. Whitehead,⁵⁴ D. Wiedner,¹⁵ G. Wilkinson,⁶³ M. Wilkinson,⁶⁸ I. Williams,⁵⁵ M. Williams,^{64,69} M. R. J. Williams,⁵⁸ F. F. Wilson,⁵⁷ W. Wislicki,³⁶ M. Witek,³⁵ L. Witola,¹⁷ G. Wormser,¹¹ S. A. Wotton,⁵⁵ H. Wu,⁶⁸ K. Wyllie,⁴⁸ Z. Xiang,⁶ D. Xiao,⁷ Y. Xie,⁷ A. Xu,⁵ J. Xu,⁶ L. Xu,³ M. Xu,⁷ Q. Xu,⁶ Z. Xu,⁵ Z. Xu,⁶ D. Yang,³ Y. Yang,⁶ Z. Yang,³ Z. Yang,⁶⁶ Y. Yao,⁶⁸ L. E. Yeomans,⁶⁰ H. Yin,⁷ J. Yu,⁷¹ X. Yuan,⁶⁸ O. Yushchenko,⁴⁴ E. Zaffaroni,⁴⁹ K. A. Zarebski,⁵³ M. Zavertyaev,^{16,u} M. Zdybal,³⁵ O. Zenaiev,⁴⁸ M. Zeng,³ D. Zhang,⁷ L. Zhang,³ S. Zhang,⁵ Y. Zhang,⁵

Y. Zhang,⁶³ A. Zhelezov,¹⁷ Y. Zheng,⁶ X. Zhou,⁶ Y. Zhou,⁶ X. Zhu,³ V. Zhukov,^{14,40} J. B. Zonneveld,⁵⁸ S. Zucchelli,^{20,d}
D. Zuliani,²⁸ and G. Zunica⁶²

(LHCb Collaboration)

¹*Centro Brasileiro de Pesquisas Físicas (CBPF), Rio de Janeiro, Brazil*

²*Universidade Federal do Rio de Janeiro (UFRJ), Rio de Janeiro, Brazil*

³*Center for High Energy Physics, Tsinghua University, Beijing, China*

⁴*Institute Of High Energy Physics (IHEP), Beijing, China*

⁵*School of Physics State Key Laboratory of Nuclear Physics and Technology, Peking University, Beijing, China*

⁶*University of Chinese Academy of Sciences, Beijing, China*

⁷*Institute of Particle Physics, Central China Normal University, Wuhan, Hubei, China*

⁸*Univ. Grenoble Alpes, Univ. Savoie Mont Blanc, CNRS, IN2P3-LAPP, Annecy, France*

⁹*Université Clermont Auvergne, CNRS/IN2P3, LPC, Clermont-Ferrand, France*

¹⁰*Aix Marseille Univ, CNRS/IN2P3, CPPM, Marseille, France*

¹¹*Université Paris-Saclay, CNRS/IN2P3, IJCLab, Orsay, France*

¹²*Laboratoire Leprince-Ringuet, CNRS/IN2P3, Ecole Polytechnique, Institut Polytechnique de Paris, Palaiseau, France*

¹³*LPNHE, Sorbonne Université, Paris Diderot Sorbonne Paris Cité, CNRS/IN2P3, Paris, France*

¹⁴*I. Physikalisches Institut, RWTH Aachen University, Aachen, Germany*

¹⁵*Fakultät Physik, Technische Universität Dortmund, Dortmund, Germany*

¹⁶*Max-Planck-Institut für Kernphysik (MPIK), Heidelberg, Germany*

¹⁷*Physikalisches Institut, Ruprecht-Karls-Universität Heidelberg, Heidelberg, Germany*

¹⁸*School of Physics, University College Dublin, Dublin, Ireland*

¹⁹*INFN Sezione di Bari, Bari, Italy*

²⁰*INFN Sezione di Bologna, Bologna, Italy*

²¹*INFN Sezione di Ferrara, Ferrara, Italy*

²²*INFN Sezione di Firenze, Firenze, Italy*

²³*INFN Laboratori Nazionali di Frascati, Frascati, Italy*

²⁴*INFN Sezione di Genova, Genova, Italy*

²⁵*INFN Sezione di Milano, Milano, Italy*

²⁶*INFN Sezione di Milano-Bicocca, Milano, Italy*

²⁷*INFN Sezione di Cagliari, Monserrato, Italy*

²⁸*Università degli Studi di Padova, Università e INFN, Padova, Padova, Italy*

²⁹*INFN Sezione di Pisa, Pisa, Italy*

³⁰*INFN Sezione di Roma La Sapienza, Roma, Italy*

³¹*INFN Sezione di Roma Tor Vergata, Roma, Italy*

³²*Nikhef National Institute for Subatomic Physics, Amsterdam, Netherlands*

³³*Nikhef National Institute for Subatomic Physics and VU University Amsterdam, Amsterdam, Netherlands*

³⁴*AGH—University of Science and Technology, Faculty of Physics and Applied Computer Science, Kraków, Poland*

³⁵*Henryk Niewodniczanski Institute of Nuclear Physics Polish Academy of Sciences, Kraków, Poland*

³⁶*National Center for Nuclear Research (NCBJ), Warsaw, Poland*

³⁷*Horia Hulubei National Institute of Physics and Nuclear Engineering, Bucharest-Magurele, Romania*

³⁸*Petersburg Nuclear Physics Institute NRC Kurchatov Institute (PNPI NRC KI), Gatchina, Russia*

³⁹*Institute for Nuclear Research of the Russian Academy of Sciences (INR RAS), Moscow, Russia*

⁴⁰*Institute of Nuclear Physics, Moscow State University (SINP MSU), Moscow, Russia*

⁴¹*Institute of Theoretical and Experimental Physics NRC Kurchatov Institute (ITEP NRC KI), Moscow, Russia*

⁴²*Yandex School of Data Analysis, Moscow, Russia*

⁴³*Budker Institute of Nuclear Physics (SB RAS), Novosibirsk, Russia*

⁴⁴*Institute for High Energy Physics NRC Kurchatov Institute (IHEP NRC KI), Protvino, Russia, Protvino, Russia*

⁴⁵*ICCUB, Universitat de Barcelona, Barcelona, Spain*

⁴⁶*Instituto Galego de Física de Altas Energías (IGFAE), Universidade de Santiago de Compostela, Santiago de Compostela, Spain*

⁴⁷*Instituto de Física Corpuscular, Centro Mixto Universidad de Valencia—CSIC, Valencia, Spain*

⁴⁸*European Organization for Nuclear Research (CERN), Geneva, Switzerland*

⁴⁹*Institute of Physics, Ecole Polytechnique Fédérale de Lausanne (EPFL), Lausanne, Switzerland*

⁵⁰*Physik-Institut, Universität Zürich, Zürich, Switzerland*

⁵¹*NSC Kharkiv Institute of Physics and Technology (NSC KIPT), Kharkiv, Ukraine*

⁵²*Institute for Nuclear Research of the National Academy of Sciences (KINR), Kyiv, Ukraine*

- ⁵³*University of Birmingham, Birmingham, United Kingdom*
⁵⁴*H.H. Wills Physics Laboratory, University of Bristol, Bristol, United Kingdom*
⁵⁵*Cavendish Laboratory, University of Cambridge, Cambridge, United Kingdom*
⁵⁶*Department of Physics, University of Warwick, Coventry, United Kingdom*
⁵⁷*STFC Rutherford Appleton Laboratory, Didcot, United Kingdom*
⁵⁸*School of Physics and Astronomy, University of Edinburgh, Edinburgh, United Kingdom*
⁵⁹*School of Physics and Astronomy, University of Glasgow, Glasgow, United Kingdom*
⁶⁰*Oliver Lodge Laboratory, University of Liverpool, Liverpool, United Kingdom*
⁶¹*Imperial College London, London, United Kingdom*
⁶²*Department of Physics and Astronomy, University of Manchester, Manchester, United Kingdom*
⁶³*Department of Physics, University of Oxford, Oxford, United Kingdom*
⁶⁴*Massachusetts Institute of Technology, Cambridge, Massachusetts, USA*
⁶⁵*University of Cincinnati, Cincinnati, Ohio, USA*
⁶⁶*University of Maryland, College Park, Maryland, USA*
⁶⁷*Los Alamos National Laboratory (LANL), Los Alamos, New Mexico, USA*
⁶⁸*Syracuse University, Syracuse, New York, USA*
⁶⁹*School of Physics and Astronomy, Monash University, Melbourne, Australia,
associated with Department of Physics, University of Warwick, Coventry, United Kingdom*
⁷⁰*Pontifícia Universidade Católica do Rio de Janeiro (PUC-Rio), Rio de Janeiro, Brazil,
associated with Universidade Federal do Rio de Janeiro (UFRJ), Rio de Janeiro, Brazil*
⁷¹*Physics and Micro Electronic College, Hunan University, Changsha City, China,
associated with Institute of Particle Physics, Central China Normal University, Wuhan, Hubei, China*
⁷²*Guangdong Provincial Key Laboratory of Nuclear Science, Institute of Quantum Matter,
South China Normal University, Guangzhou, China,
associated with Center for High Energy Physics, Tsinghua University, Beijing, China*
⁷³*School of Physics and Technology, Wuhan University, Wuhan, China, associated with Center for High Energy Physics, Tsinghua
University, Beijing, China*
⁷⁴*Departamento de Física, Universidad Nacional de Colombia, Bogota, Colombia, associated with LPNHE, Sorbonne Université,
Paris Diderot Sorbonne Paris Cité, CNRS/IN2P3, Paris, France*
⁷⁵*Universität Bonn—Helmholtz-Institut für Strahlen und Kernphysik, Bonn, Germany,
associated with Physikalisch Institut, Ruprecht-Karls-Universität Heidelberg, Heidelberg, Germany*
⁷⁶*Institut für Physik, Universität Rostock, Rostock, Germany,
associated with Physikalisch Institut, Ruprecht-Karls-Universität Heidelberg, Heidelberg, Germany*
⁷⁷*INFN Sezione di Perugia, Perugia, Italy,
associated with INFN Sezione di Ferrara, Ferrara, Italy*
⁷⁸*Van Swinderen Institute, University of Groningen, Groningen, Netherlands,
associated with Nikhef National Institute for Subatomic Physics, Amsterdam, Netherlands*
⁷⁹*Universiteit Maastricht, Maastricht, Netherlands,
associated with Nikhef National Institute for Subatomic Physics, Amsterdam, Netherlands*
⁸⁰*National Research Centre Kurchatov Institute, Moscow, Russia,
associated with Institute of Theoretical and Experimental Physics NRC Kurchatov Institute (ITEP NRC KI), Moscow, Russia*
⁸¹*National Research University Higher School of Economics, Moscow, Russia,
associated with Yandex School of Data Analysis, Moscow, Russia*
⁸²*National University of Science and Technology “MISIS”, Moscow, Russia, associated with Institute of Theoretical and Experimental
Physics NRC Kurchatov Institute (ITEP NRC KI), Moscow, Russia*
⁸³*National Research Tomsk Polytechnic University, Tomsk, Russia,
associated with Institute of Theoretical and Experimental Physics NRC Kurchatov Institute (ITEP NRC KI), Moscow, Russia*
⁸⁴*DS4DS, La Salle, Universitat Ramon Llull, Barcelona, Spain,
associated with ICCUB, Universitat de Barcelona, Barcelona, Spain*
⁸⁵*University of Michigan, Ann Arbor, Michigan, USA, associated with Syracuse University, Syracuse, New York, USA*

^aAlso at Universidade Federal do Triângulo Mineiro (UFTM), Uberaba-MG, Brazil.^bAlso at Hangzhou Institute for Advanced Study, UCAS, Hangzhou, China.^cAlso at Università di Bari, Bari, Italy.^dAlso at Università di Bologna, Bologna, Italy.^eAlso at Università di Cagliari, Cagliari, Italy.^fAlso at Università di Ferrara, Ferrara, Italy.^gAlso at Università di Firenze, Firenze, Italy.^hAlso at Università di Genova, Genova, Italy.ⁱAlso at Università degli Studi di Milano, Milano, Italy.

^j Also at Università di Milano Bicocca, Milano, Italy.

^k Also at Università di Modena e Reggio Emilia, Modena, Italy.

^l Also at Università di Padova, Padova, Italy.

^m Also at Scuola Normale Superiore, Pisa, Italy.

ⁿ Also at Università di Pisa, Pisa, Italy.

^o Also at Università della Basilicata, Potenza, Italy.

^p Also at Università di Roma Tor Vergata, Roma, Italy.

^q Also at Università di Siena, Siena, Italy.

^r Also at Università di Urbino, Urbino, Italy.

^s Also at MSU—Iligan Institute of Technology (MSU-IIT), Iligan, Philippines.

^t Also at AGH—University of Science and Technology, Faculty of Computer Science, Electronics and Telecommunications, Kraków, Poland.

^u Also at P.N. Lebedev Physical Institute, Russian Academy of Science (LPI RAS), Moscow, Russia.

^v Also at Novosibirsk State University, Novosibirsk, Russia.

^w Also at Department of Physics and Astronomy, Uppsala University, Uppsala, Sweden.

^x Also at Hanoi University of Science, Hanoi, Vietnam.